# Experimental Demonstration of a Soft X-Ray Self-Seeded Free-Electron Laser

D. Ratner,[1,*] R. Abela,[2] J. Amann,[1] C. Behrens,[1] D. Bohler,[1] G. Bouchard,[1] C. Bostedt,[1] M. Boyes,[1] K. Chow,[3]
D. Cocco,[1] F. J. Decker,[1] Y. Ding,[1] C. Eckman,[1] P. Emma,[1] D. Fairley,[1] Y. Feng,[1] C. Field,[1] U. Flechsig,[2]
G. Gassner,[1] J. Hastings,[1] P. Heimann,[1] Z. Huang,[1] N. Kelez,[1] J. Krzywinski,[1] H. Loos,[1] A. Lutman,[1]
A. Marinelli,[1] G. Marcus,[1] T. Maxwell,[1] P. Montanez,[1] S. Moeller,[1] D. Morton,[1] H. D. Nuhn,[1] N. Rodes,[3]
W. Schlotter,[1] S. Serkez,[4] T. Stevens,[3] J. Turner,[1] D. Walz,[1] J. Welch,[1] and J. Wu[1]

[1]*SLAC National Accelerator Laboratory, Menlo Park, California 94720, USA*
[2]*Paul Scherrer Institut, CH-5232 Villigen PSI, Switzerland*
[3]*Lawrence Berkeley National Laboratory (LBNL), 1 Cyclotron Road, Berkeley, California 94720, USA*
[4]*Deutsches Elektronen-Synchrotron (DESY), Notkestrasse 85, D-22607 Hamburg, Germany*
(Received 3 October 2014; published 6 February 2015)

The Linac Coherent Light Source has added a self-seeding capability to the soft x-ray range using a grating monochromator system. We report the demonstration of soft x-ray self-seeding with a measured resolving power of 2000–5000, wavelength stability of $10^{-4}$, and an increase in peak brightness by a factor of 2–5 across the photon energy range of 500–1000 eV. By avoiding the need for a monochromator at the experimental station, the self-seeded beam can deliver as much as 50-fold higher brightness to users.

The construction of x-ray free-electron lasers (FELs) driven by self-amplified spontaneous emission (SASE) has pushed the brightness of x-ray sources by a remarkable 10 orders of magnitude [1,2]. Despite the relatively monochromatic output (typically bandwidth is on the order of 0.2%–0.5% of the fundamental energy), many types of experiments benefit from even narrower bandwidth; the ability to target and measure fine energy structure in combination with femtosecond pulse length enables new opportunities in time-resolved x-ray spectroscopy. As an example, ultrafast resonant inelastic x-ray scattering can probe the evolution of low energy electronic excitations in correlated electron materials. At the Linac Coherent Light Source (LCLS), the soft x-ray (SXR) experimental hutch monochromator can select a narrow slice of the FEL bandwidth, but has diffraction efficiency of only 15%–30% and increases the focal spot size, resulting in a factor of 10 or more drop in the total brightness [3]. Moreover, some photon-hungry and time-resolved experiments cannot use a hutch monochromator and must accept the full SASE bandwidth. Rather than reducing the bandwidth after the FEL, it is preferable to reduce the FEL bandwidth itself.

The FEL amplification process ideally would begin from a well characterized, coherent "seed." However, due to a lack of external seeds at x-ray wavelengths, all current and planned x-ray FELs are SASE FELs, in which the shot noise of the electron beam itself generates the seed [4]. Harmonic seeding techniques (e.g., [5]) can convert seeds to shorter wavelengths, but performance deteriorates at photon energies beyond a few hundred eV [6]. An alternative approach to external seeding is "self-seeding," in which the FEL is split into two pieces and a monochromatic slice of the spectrum from the first portion provides the

seed for the second portion [7]. Self-seeding can be described as follows: First, the initial portion of the FEL generates relatively wide bandwidth SASE radiation. Second, a magnetic electron chicane separates the electron and photon beams; on the photon branch, a tunable monochromator selects a narrow bandwidth out of the SASE spectrum, while on the electron branch the electron chicane dispersion resets the electron beam to its initial shot noise distribution (washing out microbunching from the SASE FEL). The chicane delay also matches the path lengths of the electron and photon beams so that they overlap following the seeding monochromator. Finally, the monochromatic x rays and the electron beam then co-propagate in a second undulator line, restarting the FEL interaction from a narrow-bandwidth and near transform-limited seed.

Though originally studied for soft x rays [8], a hard x-ray variant using a diamond Bragg condition has been in use at LCLS for the last two years [9,10]. Following successful commissioning of the technically simpler hard x-ray self-seeding (HXRSS) system, a three-way collaboration between SLAC, Lawrence Berkeley National Laboratory, and the Paul Scherrer Institut formed to implement a grating-based soft x-ray self-seeding (SXRSS) project at LCLS [11]. Here, we report the experimental demonstration of self-seeding in the soft x-ray range.

The LCLS SXRSS project was designed to fit into the existing LCLS undulator hall. To preserve SASE and HXRSS operation, only a single 3.4 m undulator section could be replaced by the SXRSS components, requiring a compact design for both the seeding monochromator and chicane. The final design situated the SXRSS system in place of undulator #9, leaving as many as eight undulators
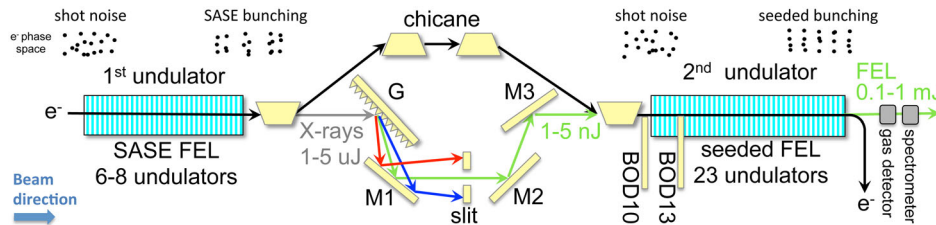
FIG. 1 (color online).    Schematic of the SXRSS system (not to scale). Shot noise from randomly distributed electrons generates 1–5 $\mu$J of relatively wide bandwidth SASE radiation in the first string of undulators (grey line). The seeding monochromator, consisting of a grating ($G$), three mirrors ($M1$, $M2$, $M3$), and an adjustable slit, selects a small bandwidth (green line) while the electron chicane directs the electron bunch around the monochromator and resets the electron beam to shot noise. Finally, the overlap diagnostics (BOD10 and BOD13) coalign electrons and monochromatic x rays in the second half of the FEL. Pulse energies are shown for a nominal electron bunch with a charge of 150 pC, and duration of 100 fs, but other parameter ranges are also possible.

upstream of the seeding monochromator to generate the seed, and 23 downstream undulators to saturate and maximize the seeded FEL power.

The SXRSS system consists of an electron chicane and x-ray monochromator (Fig. 1), and a pair of beam overlap diagnostics (BODs) located further downstream. Here, we give an overview of the system components, but a detailed description can be found in [12,13]. The four-dipole electron chicane serves three purposes: steering electrons around the x-ray monochromator optics, delaying the electrons to match the x-ray delay in the seeding mono-chromator, and washing out microbunching from the initial SASE FEL. Because of the limited space available, the electron beam travels within a cm of the first and fourth x-ray optical surfaces. Rather than construct thin optics, a hole through the thick optical substrate provides safe passage of the electron beam through the optics [12]. The chicane can produce a maximum delay of approximately ∼1 ps, with a minimum delay of 0.5 ps in seeded mode to protect the optics. With a relative slice energy spread in the electron bunch of a few $10^{-4}$, the temporal dispersion of the chicane washes out any microbunching at x-ray wavelengths.

The seeding monochromator contains four platinum-coated optical elements: a variable line spacing toroidal grating, two flat mirrors ($M1$ and $M3$), and a spherical mirror ($M2$) (Fig. 2). Motors insert or extract each optic
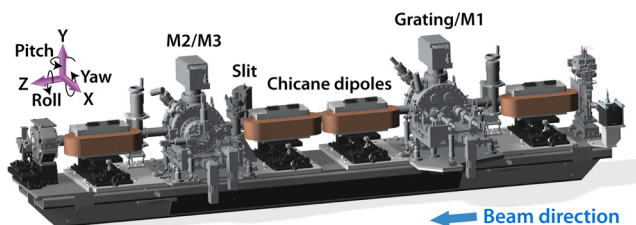


FIG. 2 (color online).    Computer aided design model of the final SXRSS design showing both the optics housing (Grating/$M1$, Slit, and $M2$/$M3$) and the electron chicane. In this figure, electrons move right to left to show the details of the optics chambers. The overlap diagnostics are further downstream.

remotely. A fifth element, a variable size slit, can be inserted between $M1$ and $M2$ to aid with alignment. (The slit is actually not needed while seeding, because only the narrow spectral slice that copropagates with the electron beam can drive seeding. Effectively, the electron beam itself acts as a "slit.") The toroidal grating provides the dispersion of the monochromator and also focuses the beam vertically into undulator #10 and horizontally through the slit. The remotely adjustable pitch of $M1$ determines which wavelength passes through the mono-chromator along the electron beam path; $M1$ pitch is the only optic movement required to scan the seeded FEL x-ray wavelength. The final optics then focus ($M2$) and overlap ($M3$) the x-ray beam with the electron beam in undulator #10. Unlike hard x-ray self-seeding, where the seed passes directly through a diamond crystal, SXRSS requires trans-verse alignment of the x rays and electrons. The slit and the two BODs help overlap the electron and photon beams and seed the FEL. Seeding is optimized by centering the seeded wavelength within the SASE bandwidth ($M1$ pitch), and maximizing both transverse overlap (grating $Y$, and $M3$ $X$, roll, and pitch), and temporal overlap (magnetic chicane strength) of the x rays and electrons. Details of the overlap and alignment procedure are given in the Supplemental Material [14].

The power in the seed pulse must be sufficient to overcome SASE startup but low enough to avoid damage to the optics. An estimated 0.15% of the SASE radiation incident on the grating is available for seeding, requiring at least 1 mJ/cm$^2$ fluence at normal incidence for a nominal 100 fs, 2 kA electron bunch. Fluence above 750 mJ/cm$^2$ can damage the grating, so the incident SASE is limited to 30 mJ/cm$^2$ [15]. Though the damage threshold is accept-able for current operation, improvements may be necessary to avoid damage in a high repetition rate machine. The damage considerations are described in more detail in the Supplemental Material [14].

A gas detector [16] and grating spectrometer [3] measure the final seeded FEL energy and spectrum, and both diagnostics can measure seeding at different positions along the undulator line [17]. The grating spectrometer,

TABLE I.　Parameters of current seeding operation for a 50 fs pulse using the slotted foil [19]. SASE pulse energy assumes optimized, nominal operation with 50–100 fs pulse length. Brightness comparisons assume a hutch monochromator filters the SASE ("filt."). The seeded beam can be used directly or filtered by a hutch monochromator to remove shoulders.

| SXRSS performance | |
| --- | --- |
| Photon energy range | 500–1000 eV |
| SASE resolving power, average | ~150 |
| SASE resolving power, single shot | ~300 |
| Seeded resolving power | 2000–5000 |
| Seeded resolving power, single shot | 2500–6000 |
| Average power ratio: seeded vs SASE | 0.1–0.3 |
| Maximum power ratio: seeded vs SASE | ~1 |
| rms pulse energy jitter (on-energy shots) | 50% |
| rms pulse energy jitter (all shots) | 100% |
| Brightness ratio: filt. seeded vs filt. SASE | 2–5 |
| Brightness ratio: seeded vs filt. SASE | 20–50 |

located in the SXR hutch, records single-shot seeded spectra with a resolution of 80 meV at 900 eV photon energy, beyond the expected resolving power of the seeding monochromator. Deep in saturation, the SASE FEL overtakes seeding, so it is preferable to setup seeding using only 10 of the 23 undulators down stream of the seeding monochromator.

Self-seeding has been observed across the nominal photon energy range of 500–1000 eV, with typical performance described in Table I. Figure 3 shows a comparison between the seeded spectra and the optimized SASE configuration (all undulators, seeding optics extracted).
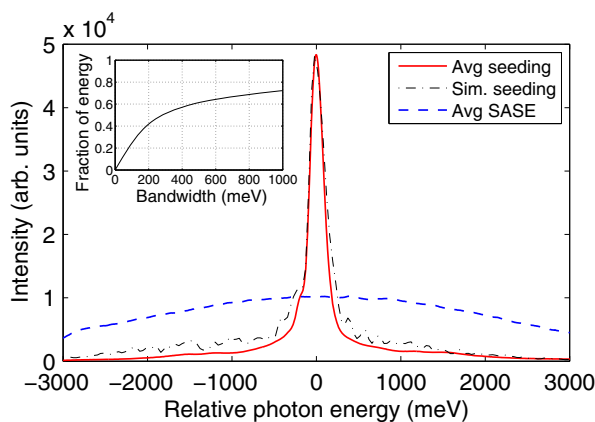


FIG. 3 (color online).　Comparison of seeded (solid red line) and SASE (dashed blue line) spectra at 930 eV for 10 000 shot averages, and seeded simulation (sim.) averaged over 30 shots (dotted-dashed black line). Both seeded and SASE spectra use the slotted foil to produce a 50 fs beam [19]. Seeded spectra are taken after undulator #25 and with the slit retracted. SASE spectra use an optimized configuration with all undulators. Inset shows the fraction of FEL energy contained within an integrated bandwidth when seeding.

Start-to-end Genesis simulations [18] agree with measurements. The seeded spectra exclude the final eight undulators, which primarily increase the undesirable SASE background. In the given spectra, the FWHM bandwidth of 175 meV contains approximately 40% of the total pulse energy. Some experiments may benefit from using the full undulator line, but the proportion of energy outside the seeding bandwidth will increase. Figure 4 shows SASE and seeded FEL gain, which matches simulations.

The peak brightness of the self-seeded FEL (defined as $mJ/s/m^2/0.1\%$ bandwidth) is larger than that of optimized SASE by a factor of 2–5. For some narrow bandwidth applications, however, it is more relevant to compare the peak brightness of the full, unfiltered self-seeded beam with the brightness of the SASE beam filtered through a hutch monochromator. When including monochromator losses and focal size growth, the unfiltered seeded beam is up to 50 times brighter than the filtered SASE for the same FWHM bandwidth. Note that using the seeded beam without a hutch monochromator may require a setup with fewer undulator sections (to produce a cleaner spectrum) at the cost of reducing the final peak power by a factor of ~2.

The central SASE wavelength is determined by the electron energy, and the wavelength can jitter by as much as 0.4% shot to shot. By comparison, the seeded wavelength is determined by the $M1$ pitch, independent of the electron energy. Figure 5(a) shows single-shot spectra, with shot-to-shot jitter of approximately 100 meV rms, corresponding to wavelength stability of $10^{-4}$. Though small compared to SASE, the jitter does broaden the average seeded spectrum: while the single-shot bandwidth is 155 meV, wavelength jitter broadens the average bandwidth to 180 meV FWHM (Fig. 3). (Both values include
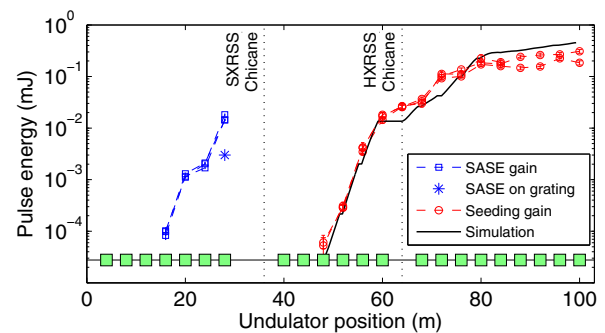


FIG. 4 (color online).　Gain length scans showing SASE growth before the seeding monochromator (blue squares, three scans) and seeding growth afterwards (red circles, three scans). During seeded operation, undulator #1 is detuned to keep pulse energy on the grating below 5 μJ (blue star). Black line shows simulated seeding. Green boxes show undulators inserted during seeding; undulator #8 is removed to protect the grating, and undulators #9 and #16 were replaced by the self-seeding chicanes. Measured gain lengths for SASE (~2 ± 0.2 m) and seeding (~1.7 ± 0.2 m) match simulations. All measurements taken with the gas detector.
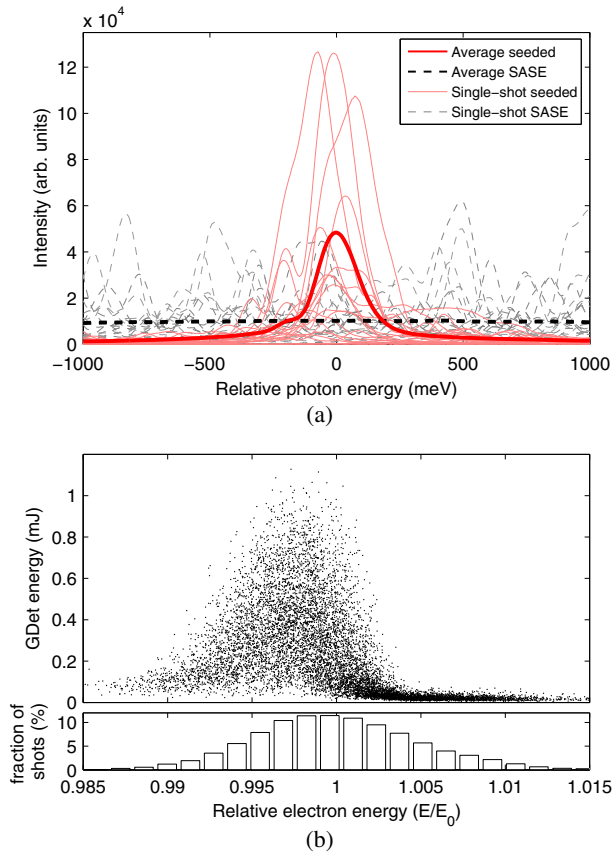
FIG. 5 (color online).    Jitter of the seeded mode for 50 fs pulse at
930 eV. (a) A comparison of 20 single-shot seeded (solid light red
lines) and SASE (dashed grey lines) spectra shows fluctuations in
both peak brightness and central seeded wavelength. Bold lines
show average performance for both seeding and SASE. (b) A
"mustache" scatter plot shows the FEL pulse energy from the gas
detector (GDet) vs measured electron bunch energy for individual
shots at 930 eV. (Average electron energy is 4.3 GeV.) Histogram
at bottom shows the jitter of the central electron beam energy. The
seeding monochromator was set slightly below the average
electron energy to match the best lasing condition.

corrections for the estimated 80 meV spectrometer reso-
lution.) With a transmissive spectrometer upstream of the
experimental station, it would be possible to remove the
wavelength jitter by sorting shots in postprocessing; a
transmissive shot-by-shot spectrometer is currently under
development. Possible causes of wavelength jitter include
vibrations changing $M1$ pitch, transverse orbit fluctuations
of the electrons (which change the seed wavelength), and
changing electron phase space (which may alter the wave-
length after seeding) [20]. Measured fluctuations in orbit
(~1 $\mu$rad) and phase space (~1 MeV/mm) are consistent
with the observed jitter.

The seeded wavelength is fixed by the monochromator
$M1$ angle, so the electron energy must be set such that the
seeded wavelength is in the center of the FEL gain
bandwidth. However, the electron energy jitters, and for
many shots, the seeding monochromator wavelength lies

outside the gain region of the FEL and the electrons cannot
be seeded. Figure 5(b) shows the total x-ray pulse energy as
a function of measured electron bunch energy; for this
example, 45% of the shots fall outside the FWHM of the
seeded region. Efforts to reduce electron energy jitter are
ongoing, and can potentially increase the average seeded
power by a factor of 2. Considering only on-energy shots,
the seeded pulse energy has 50% fluctuations, compared to
25% fluctuations for SASE. (Note that the SASE fluctua-
tions in both cases were larger than usual due to the use of
the slotted foil.)

The seeding monochromator grating produces multiple-
order reflections, of which the first is strongest and used for
self-seeding operation. The second order diffraction also
has sufficient power to drive seeding. Despite having
stronger dispersion, it does not provide higher resolving
power due to diffraction effects, but in principle can access
shorter wavelengths than the first order. By increasing $M1$
pitch angle in the seeding configuration, we have observed
seeding driven by the second order, but have not tried to
optimize second order seeding at this time.

Upgrades to the self-seeding mode will focus on improv-
ing performance after saturation and reducing the pedestal
and shoulders of the seeded spectrum. At present the slit
has been used primarily for alignment, but in principle, with
an optimized setup, the narrowest slit (3 $\mu$m wide) could
increase the resolving power. Tapering beyond undulator
#25 may require modifications to the undulator configura-
tion. Two-color self-seeding has been demonstrated for the
HXRSS system [21] and in principle two-color operation
is also possible for SXRSS. However, unlike hard x rays,
simultaneous two-color operation at soft x rays will require
hardware changes. Two-color operation with only one color
seeded is possible by detuning a portion of the undulators
[22] or with two-bunch operation [23]. Seeded radiation
with polarization control will be available following instal-
lation of the Delta undulators [24].

Development of soft x-ray self-seeding will continue
through 2015 as the SXRSS mode is prepared for user
operation. As of August 2014, we have produced average
resolving power of 2000–5000 with wavelength stability
of $10^{-4}$ across the designed energy range 500–1000 eV.
Average brightness is approximately a factor of 2–5 higher
and resolving power is approximately a factor of 20 higher
than in optimized SASE configuration. Self-seeding with-
out a hutch monochromator will provide a factor of 20 or
more increase in brightness compared to SASE operation
with a hutch monochromator. Future work will focus on
improving electron stability to increase the average bright-
ness and reducing the pedestal of the x-ray spectrum to
optimize user operation without a hutch monochromator.
Taper studies are ongoing and simulations indicate an
improved taper could increase brightness as well as peak
power. Future work may eventually extend the operating
range to 300–1200 eV.

PHYSICAL REVIEW LETTERS

[*] dratner@slac.stanford.edu

[1] P. Emma *et al.*, Nat. Photonics **4**, 641 (2010).

[2] H. Tanaka *et al.*, Nat. Photonics **6**, 540 (2012).

[3] P. Heimann *et al.*, Rev. Sci. Instrum. **82**, 093104 (2011).

[4] R. Bonifacio, C. Pellegrini, and L. M. Narducci, Opt. Commun. **50**, 373 (1984).

[5] L. H. Yu, Phys. Rev. A **44**, 5178 (1991).

[6] E. Allaria *et al.*, Nat. Photonics **7**, 913 (2013).

[7] J. Feldhaus, E. Saldin, J. Schneider, E. Schneidmiller, and M. Yurkov, Opt. Commun. **140**, 341 (1997).

[8] Y. Feng, J. Hastings, P. Heimann, M. Rowen, J. Krzywinski, and J. Wu, in *Proceedings of the 32nd International Free Electron Laser Conference (FEL 10), Hilton Malmöö City, Sweden, 2010* (FEL-MMX Sverige, Sweden, 2010).

[9] G. Geloni, V. Kocharyan, and E. Saldin, J. Mod. Opt. **58**, 1391 (2011).

[10] J. Amann *et al.*, Nat. Photonics **6**, 693 (2012).

[11] Y. Feng *et al.*, in *Proceedings of the 34th International Free Electron Laser Conference (FEL 12), Nara, Japan, 2012* (JACoW, Geneva, 2012).

[12] D. Cocco *et al.*, Proc. SPIE-Int. Soc. Opt. Eng. **8849**, 88490A (2013).

[13] H. Loos, P. Montanez, D. Ratner, and J. Hastings, LCLS Physics Specifications for the SXRSS Beam Overlap Diagnostics, SLAC Report No. SLAC-PUB-16073, 2014 (unpublished).

[14] See Supplemental Material at http://link.aps.org/supplemental/10.1103/PhysRevLett.114.054801 for more detailed description of commissioning, damage concerns, and diagnostics.

[15] J. Krzywinski, D. Cocco, S. Moeller, and D. Ratner, Damage Threshold of Platinum Coating Used for Optics for Self-Seeding of Soft X-ray Free Electron Laser, SLAC Report No. SLAC-PUB-16096, 2015.

[16] S. Hau-Riege, R. Bionta, D. Ryutov, and J. Krzywinski, J. Appl. Phys. **103**, 053306 (2008).

[17] D. Ratner *et al.*, in *Proceedings of the 31st International Free Electron Laser Conference (FEL 09), Liverpool, UK* (STFC Daresbury Laboratory, Warrington, 2009).

[18] S. Reiche, Nucl. Instrum. Methods Phys. Res., Sect. A **429**, 243 (1999).

[19] P. Emma, K. Bane, M. Cornacchia, Z. Huang, H. Schlarb, G. Stupakov, and D. Walz, Phys. Rev. Lett. **92**, 074801s (2004).

[20] A. Marinelli, C. Pellegrini, L. Giannessi, and S. Reiche, Phys. Rev. ST Accel. Beams **13**, 070701 (2010).

[21] A. A. Lutman *et al.*, Phys. Rev. Lett. **113**, 254801 (2014).

[22] A. A. Lutman, R. Coffee, Y. Ding, Z. Huang, J. Krzywinski, T. Maxwell, M. Messerschmidt, and H.-D. Nuhn, Phys. Rev. Lett. **110**, 134801 (2013).

[23] A. Marinelli *et al.* (to be published).

[24] H.-D. Nuhn *et al.*, in *Proceedings of the 35th International Free Electron Laser Conference (FEL 13) New York, 2013* (JACoW, Geneva, 2013).